Exploring the Architectural Trade Space of NASAs Space Communication and Navigation Program

Marc Sanchez, Daniel Selva, Bruce Cameron, Edward Crawley
Massachusetts Institute of Technology
77 Massachusetts Ave 33-409
Cambridge, MA 02139
617-682-6521
{msnet,dselva,bcameron,crawley}@mit.edu

Antonios Seas, Bernie Seery
NASA Goddard Space Flight Center
8800 Greenbelt Road
Greenbelt, MD 20771
301-286-7979
{Antonios.A.Seas, Bernard.D.Seery}@nasa.gov

Abstract— **NASAs Space Communication and Navigation (SCaN) Program is responsible for providing communication and navigation services to space missions and other users in and beyond low Earth orbit. The current SCaN architecture consists of three independent networks: the Space Network (SN), which contains the TDRS relay satellites in GEO; the Near Earth Network (NEN), which consists of several NASA-owned and commercially operated ground stations; and the Deep Space Network (DSN), with three ground stations in Goldstone, Madrid, and Canberra.**

The first task of this study is the stakeholder analysis. The goal of the stakeholder analysis is to identify the main stakeholders of the SCaN system and their needs. Twenty-one main groups of stakeholders have been identified and put on a stakeholder map. Their needs are currently being elicited by means of interviews and an extensive literature review. The data will then be analyzed by applying Cameron and Crawley's stakeholder analysis theory, with a view to highlighting dominant needs and conflicting needs.

The second task of this study is the architectural tradespace exploration of the next generation TDRSS. The space of possible architectures for SCaN is represented by a set of architectural decisions, each of which has a discrete set of options. A computational tool is used to automatically synthesize a very large number of possible architectures by enumerating different combinations of decisions and options. The same tool contains models to evaluate the architectures in terms of performance and cost. The performance model uses the stakeholder needs and requirements identified in the previous steps as inputs, and it is based in the VASSAR methodology presented in a companion paper.

This paper summarizes the current status of the MIT SCaN architecture study. It starts by motivating the need to perform tradespace exploration studies in the context of relay data systems through a description of the history NASA's space communication networks. It then presents the generalities of possible architectures for future space communication and navigation networks. Finally, it describes the tools and methods being developed, clearly indicating the architectural decisions that have been taken into account as well as the systematic approach followed to model them. The purpose of this study is to explore the SCaN architectural tradespace by means of a computational tool. This paper describes the tool, while the tradespace exploration is underway.

978-1-4673-1813-6/13/$31.00 ©2013 IEEE.
[1] IEEEAC Paper #2451, Version 4, Updated 1/5/2013.

TABLE OF CONTENTS

1. INTRODUCTION

Background

Early history— In 1956, the Space Studies Board of the National Academy of Sciences approved a plan by the Smithsonian Astrophysical Observatory to establish an optical tracking network to track the first American satellites [1]. In a few years, 12 optical ground stations were built around the world. The utility of these stations was limited due to the low degree of automation in the acquisition of targets.Microwave interferometric satellite tracking stations (Minitrack) were also developed in the 1950's. Minitrack was the primary TT&C network for NASA during most of the late 1950's and early 1960's. Explorer 1 and Vanguard 1 were successfully launched in 1958 and tracked through the Minitrack VHF tracking network.

NASA was also created in 1958, accelerating the pace of space exploration and starting ambitious manned and unmanned programs. After Alan Shephard became the first American in space in 1960 the launch rate of unmanned and manned spacecraft started to grow, thus imposing tighter requirements on Minitrack. In particular, the needs for more sophisticated telemetry and control for scientific and application satellites became clear. This caused the development of a higher performance Satellite Tracking and Data Acquisition Network (STADAN) in the early 1960's, which used 12-meter and 26-meter S-band antennas for TT&C. Active tracking systems such as GRARR were also developed as the passive interferometric systems were unable to track satellites

in highly eccentric or high altitude orbits. Satellite Automatic Tracking Antennas (SATAN) were installed in order to enable data downlink for high data rate spacecraft. As NASA started to launch satellites into polar orbits, new ground stations such as Tananarive were added to the network.

The Manned Space Flight Network (MSFN) was created to support the Mercury, Gemini, and Apollo manned programs. With STADAN and MSFN being actively operated, the use of the Minitrack network tampered off.

In 1971, the STADAN and MSFN networks were consolidated into a single network, the Spaceflight Tracking and Data Network (STDN). It then became clear that using ground assets exclusively was not enough to meet the user requirements (especially those of manned spaceflight) due to line-of-sight constraints. The solution to this was to incorporate space assets to the network, namely the Space Network (SN), whihc includes a constellation of GEO satellites known as the Tracking and Data Relay Satellite System (TDRSS), and the supporting ground terminals in White Sands and Guam.

The first generation of TDRSS was conceived in the early 70's to replace the network of ground stations that NASA used for their manned spaceflight program. TDRSS' maiden launch occured on April 4 1983. Seven first generation TDRS satellites (TDRS-1 through TDRS-7) were launched between 1983 and 1995 into GEO orbits (although TDRS-2 never reached orbit, as it was destroyed in the Challenger disaster). The second generation of TDRSS started with the launch of TDRS-8 in 2000, with the more satellites (TDRS-9 and TRDS-10 launched in 2002). In turn, the launch of the first third generation TDRSS satellite (TDRS-K which will become TDRS-11) is currently scheduled for end of 2012. In its current implementation, the TDRSS space segment has three primary spacecraft in GEO locations at any given time, namely 40deg W (TDE), 170deg W (TDW), and 275deg W (TDS) to provide global continuous coverage of most latitudes - coverage on the polar region is reduced due to the use of equatorial orbits.

The ground segment of STDN became the Near Earth Network (NEN). The current NEN consists of six NASA-operated and ten commercially operated ground stations featuring a broad range of antennas between 4 and 18 meters.

The last element of the network is the Deep Space Network, which was also created in the late 1950's with the goal of providing TT&C services to unmanned interplanetary missions. The DSN was managed by JPL for NASA since its inception, and currently has three ground stations in Goldstone, Canberra, and Madrid with several 34-meter and one 70-m parabolic antennas per site.

The SCaN program—In 2006, the SCaN program was assigned management and systems engineering responsibilities for the SN, the NEN, and the DSN. The goal of this change was to ensure that the architecture of the three formerly independent networks would evolve in a synergistic way to converge into a unified network that meets the needs of all user communities. Since then, the SCaN program office has started a study to explore architecture options for the SCaN system. Some preliminary architectural documents have already been produced by the SCaN program office. This piece of research is part of this overall architectural effort, and has as its primary goal to identify driving architectural decisions and trades to inform the system architecting process.

2. ARCHITECTURE OF SPACE COMMUNICATION AND NAVIGATION NETWORKS

The following subsections provide some background about the architecture of a space communication and navigation network. The intent of this section is to give a broad introduction to the field and motivate the architectural decisions that will be described in section 6.

Orbit and constellation design

The space segment configuration defines how the network nodes are distributed in one or more constellations around the Earth. It can be generically classified depending on the altitudes at which the relay satellites are placed: LEO orbit, MEO orbit, GEO orbit and HEO orbit.

LEO constellations are composed of a large number of spacecrafts flying in polar or inclined circular orbits. They achieve global coverage by coordinately spacing the spacecraft so that when a satellite loses line of sight there is at least another one that comes into view. The main advantage of LEO constellations is their limited distance to the Earth surface, from 160 km to 2,000 km. This decreases the power requirements for the space to ground links, minimizes the communication propagation delays and reduces the launch costs. Nevertheless, the small orbital periods (from 90 to 130 min approximately) limit the contact windows between the relay satellites and the ground stations to 10-15 min thus reducing the volume of data that can be successfully returned. Similarly, a relay system based on LEO satellites would suffer from short satellite-to-customer contact windows and would require complex tracking and acquisition mechanisms. To mitigate this problem, past systems have usually chosen low frequency bands (L, S bands) where antennas have low gain (or almost omnidirectional) radiation patterns. However, these low gain antennas can only provide limited data rates (tens to hundreds of kbps) to support MSS[2] and TT&C[3] services.

In contrast, GEO constellations place relay satellites at zero or near zero inclined circular orbits at an altitude of 35,786 km. Full time coverage for LEO spacecrafts can be achieved through only three $\approx 120\,\mathrm{deg}$ separated satellites with a $25 - 35\,\mathrm{deg}$ FOV[4]. As a result, the contact time between the LEO spacecraft and the relay satellite doubles to 20-25 minutes thus increasing the data volume that can be sent over a contact. Moreover, since each relay satellite appears to be nearly static from the Earth surface, GEO constellations usually take advantage of high frequency bands (Ku, Ka-band) where antennas are highly directional. By implementing pointing and tracking capabilities they can provide trunk links at high data rates (tens to hundreds of Mbps) and therefore support Internet-based services or science data return services. Nevertheless, the high altitude at which each satellite is placed has also negative implications: first, it increases the propagation delays to 250 ms thus lowering the QoS[5] for real-time services; second, it increases the spacecraft cost due to larger power and antenna requirements so as to compensate for higher free space losses; and third, it augments the launching costs.

MEO orbits comprise all altitudes between 2,000 and 35,786

[2]Mobile Satellite Services
[3]Telemetry, Tracking and Command
[4]Field Of View
[5]Quality of Service

km although most constellations are placed between 19,000 and 25,000 km. This is due to two main reasons: the orbital period at these altitudes is 12 hours approximately; the inner and outer Van Allen radiation belts have peaks of intensity both below and above them. As a result, MEO constellations are a compromise option between LEO and GEO constellations. They take advantage of longer contact windows and shorter distance for Earth to ground links. However, since the spacecraft are still moving with respect to the Earth surface global coverage requires placing a relatively large set of satellites at high altitudes.

Finally, HEO constellations are a less common alternative that can provide full coverage to polar regions over one hemisphere. They are primarily used in for countries where a large portion of the territory is placed at high latitudes and therefore cannot be served with GEO satellites. In this configuration, satellites are placed in inclined highly elliptical orbits that have their perigee placed over the desired service zone. At least two coordinated spacecrafts are required in order to provide continuous coverage.

Design of communication payloads

A relay satellite can be modeled as a set of communication payloads that provide point-to-point connectivity with customer spacecraft. The technologies implemented in these communication payloads determine not only the capacity of the system but also how it has to operate so as to provide a given QoS.Three main high level categories can be envisioned:

(1) Bent-pipe payloads: Relay satellites operate as a mirror that reflects the signal from the source to the destination. The general structure of the payload consists of a RF front-end with an antenna, a low noise amplifier (LNA) and a mixer to down convert the signal to an intermediate frequency (IF). Next, the signal is filtered, frequency-translated, power-amplified and routed to the antenna that will retransmit the signal to the destination.

(2) OBP[6] circuit-switched payloads: The satellite demodulates the incoming signal in order to recover and process the received bit stream. This strategy has two main advantages: first, it improves the performance of an end-to-end communication path between 3 and 5 dB compared to a traditional bent-pipe architecture [2]; second, it allows implementing routing protocols that autonomously determine the next hop for a given connection. Moreover, link resources are allocated at the beginning of the transmission and remain dedicated until it ends regardless of the burstiness of the information being sent.

(3) OBP packet-switched payloads: The satellite emulates the behavior of an Internet node. Information flows through the network as packets that can be independently routed from source to destination. Link capacities can be optimally shared among multiple transmissions through statistical multiplexing. As a result, it has been proven that for a given blocking probability the link capacities can reduced by a 1.2 to 3 depending on traffic burstiness and the network size [3].

The design of the communication payloads also determines how the end users will be pointed and tracked in order to maintain a communication link. As previously stated, low data rate applications can rely on low gain antennae that do not need pointing and tracking capabilities. However, the majority of high data rate services require directional antennae in order to provide enough gain to close the link budget. In this scenario, two antenna configurations are possible. Single beam antennae concentrate the transmission power on a specific region of the space where one end user is located. The established link is always dedicated and therefore there is no need for implementing multiple access mechanisms. On the other hand, multiple beam antennae can produce a set of independent beams each one with a particular area of coverage. The system is designed to support more than one user at once and therefore a multiple access mechanism is put together in order to coordinate the transmissions and avoid undesired interferences. The result is a system that has greater overall connectivity (more users can connect to the network though at limited data rates) and lower costs compared to a large number of single accesses.
Choosing between single access and multiple access payloads depends primarily on the number users that must be supported at once and the data rates that their services will demand. High data rate services such as science data return will typically use single accesses to support their transmissions. In turn, low data rate services such as command or telemetry will preferably rely on a multiple access payload.

Ground segment

The ground segment is composed of a set of facilities that communicate with the relay satellites and act as interface points between the space and terrestrial domain. Its architecture is highly influenced by the constellation and payload design of the space segment.

Defining the architecture of the ground segment implies considering two factors: how many facilities are needed and where should they be placed; what technologies should be used at each location.

The locations where to place ground stations depend on both technical and non-technical factors. Technical factors are usually related to the location and configuration of the spacecraft as well as the amount of information that needs to be received. For instance, GEO constellations typically require 1-4 locations since the spacecraft are in a fixed position with respect to the Earth surface. As an example, NASA's TDRSS can provide global coverage with only two ground stations, the White Sands Complex in New Mexico (US) and the Guam Remote Ground Terminal in the Pacific Ocean. Alternatively, LEO and MEO constellations might need to use a large network of ground stations because they continually lose and acquire line of sight with them. This is usually mitigated by using intersatellite links in order to route the information to a satellite that is in view of a ground station. On the other hand, non-technical factors are related to economic, strategic and diplomatic issues due to the facilities being located overseas. Although this might not represent a challenge in the design phases of the system, it may dramatically increase the operational cost of the ground segment and even ban some optimal locations.

The number and type of antennas to be placed depends primarily on the expected amount of connections, data rates and distances for space to ground links. GEO constellations typically use 10-20 meter parabolic antennas that have enough gain to compensate for high free space losses. Alternatively, LEO systems can use smaller antennas (5 to 15 meters) but require greater mobility in order to properly track the relay satellites. Lastly, optical links might place additional constraints in the design of the ground segment. Since the communication is only possible when there are

[6] Onboard Processing

no clouds between the satellite and a ground station, the overall availability of the space to ground communication can only be achieved through *ground station diversity*. In this strategy, multiple facilities are placed so that they can potentially support the same space to ground link. When a particular ground station is covered by a cloud, the link is automatically switched to another one that has free line of sight.

Communication technologies and protocols

Once the network configuration and topology have been designed it is necessary to define a stack of protocols that optimize the network performance. This is typically done by selecting a set of protocols for each layer of the OSI reference frame.

The physical layer defines the electrical and physical specifications of the communication between two nodes of the network. Selecting an architecture requires indicating the frequency bands and modulations used to transform the data bit streams into RF signals. Together with the antenna characteristics, these decision determine the data rates achievable on a particular link. Current space systems typically operate at L, S, C, X, Ku and Ka-bands according to the international and national RF spectrum regulations. Nevertheless, the need for increasing data rates is fostering the deployment of payloads using higher frequency bands (Ka, W-band and optical) to take advantage of greater communication bandwidths. Similarly, most current systems use well known BPSK and QPSK modulations to encode the bit stream. Future systems will implement higher efficient modulation schemes such as GMSK, OQPSK, SOQPSK, 8-PSK and QAM.

For the data link layer, decisions regarding the appropriate forward error correcting and multiple access scheme must be made. Legacy systems typically rely on Reed-Solomon, BCH and convolutional codes or remain uncoded depending on the link characteristics and how sensitive are the data being sent. New systems will move forward to turbo and Low Density Parity Check (LDPC) codes that offer a superior coding gain compared to traditional techniques. On the other hand, multiple access schemes will continue to use FDMA, TDMA and CDMA (or a combination of those) as the main approaches to coordinate multiple users transmitting at the same time. It is also expected that new systems will implement DAMA[7] instead of traditional statically assigned schemes.

Finally, the network layer indicates how data are routed through the nodes. Systems operating under a bent-pipe architecture do not implement this layer since routing decisions are computed on the ground beforehand and uploaded to the relay satellites. Alternatively, newer systems are already implementing off-the-shelf network and transport protocols that open the path and foster the implementation of packet-switched networks similar to the terrestrial Internet. As an example, the CCSDS[8] has already published the *Space Communications Protocol Specifications*, an extension of the existing Internet protocols for space environments.

3. LITERATURE REVIEW

In this section, we review the state-of-the-art of computational tools that have been used in the past in the context of early architectural studies, both of space communication networks and in general.

Computational Tools for Architecting Space Communications Networks

Several computational tools have been developed for modeling and evaluating the performance of space communication networks. Two main strategies have been identified:

(1) Tools that rely on a network simulator that uses a discrete event engine to generate the traffic. Each node has a set of protocols that define the specifics of the information being sent over the network.
(2) Tools that abstract the network data flows and treat them as an amount of data rate that is needed in order to achieve successful communication. The goal of the simulation is to understand if the network capacity can support a certain load given the topology and routing policies.

References [4], [5], [6] fall under category (1). They describe NASA's developed tools for modeling a space communication network. In particular, their software combines STK and QualNet in order to simulate the end-to-end performance of the network. The latter is used for the upper layers of the OSI reference frame (application to data link) while the former is constantly queried and computes the physical properties of the RF and optical links.

On the other hand, [7], [8], [9] present frameworks that follow approach (2). They implement either shortest path algorithms or multicommodity flow algorithms in order to route data flows and estimate the overall network capacity.

Computational Tools for Architecting Other Systems

Computational tools are used in system architecting for several purposes:

(1) To describe different aspects or views of a system architecture using models (e.g. SysML [10])

(2) To simulate the operational behavior of a system architecture using models (e.g. OPCAT [11])

(3) To optimize a system architecture (e.g. OPN [12])

This paper focuses on tools that fall in the third category, i.e. tools developed to optimize a system architecture, or in other words, to explore the architectural tradespace. These tools have a way of encoding a system architecture in an enumerable data structure (e.g., an array). At the very least, these tools need to be able to:

1) Enumerate a tradespace of architectures, usually defined by means of a set of architectural variables and their corresponding range of allowed values

2) Evaluate architectures based on a set of metrics or figures of merit (e.g., cost, performance)

3) Down-select architectures based on a set of criteria (e.g., non-dominatedness in the Pareto sense).

Tools used to explore small tradespaces can usually fully enumerate the tradespace. For larger tradespaces that cannot be fully explored, optimization algorithms become necessary. Within these, heuristic algorithms are typically used, as they

[7]Demand Assigned Multiple Access
[8]Consultative Committee for Space Data Systems

are effective in handling non-convex multi-objective combinatorial optimization problems [13].

An exhaustive literature of computational tools for system architecting can be found in [14].

4. RESEARCH GOALS AND PAPER STRUCTURE

Research goals

The goal of this study is to develop a tool to support the system architecting phase of the SCaN system. A preliminary stakeholder analysis will provide information about stakeholders and their needs and corresponding requirements on the system, which will be used as inputs to the tool. The computational tool is largely based on the VASSAR framework presented in a companion paper [15]. VASSAR is a general methodology that assess the value of a system architecture using rule-based systems. The main idea behind VASSAR is that value can be assessed by systematically comparing the capabilities of the system architecture with the stakeholder requirements. A very detailed description of the VASSAR framework is provided in [15].

Paper structure

The rest of the paper is organized as follows: Section 5 gives an overview of the efforts related to the stakeholder analysis. Section 6 describes the tradespace exploration tool; it starts by defining how architectural decisions are encoded into variables, and then goes on to briefly explain how architectures are automatically enumerated. The rest of this section is devoted to the detailed description of the cost and performance metrics used by the tool. Finally, in Section 7, the current status of the tool development is summarized, and the next steps are outlined.

5. STAKEHOLDER ANALYSIS

The purpose of the stakeholder analysis task is to identify the relevant stakeholders against which the generated architectures should be graded, and to define the needs against which the architecture performance will be evaluated. Prior stakeholder analysis of NASAs exploration goals and also of NOAAs earth observation program are important progenitors for this study [16], [17], [18].

The timeframe around which this study is scoped is 2020-2030, which poses two inherent challenges. The first challenge is that in many cases customers needs are a function of the capability of the system. For example, although TT&C data rates can sometimes be known and fixed well in advance, many customers would benefit from increased data rates should they become available. The second challenge is that technology of the customer spacecraft will continue to evolve, while the relay architecture will be determined. Where possible, this model attempts to determine stakeholder satisfaction as a function of performance, rather than enumerating binary requirements.

Identification of stakeholders proceeded largely from the existing customer base of TDRS relay users, with several important additions. An explicit decision was made to decompose the system by stakeholder communities (such as Earth Science), rather than by mission. The authors felt this would mitigate missions as a source of uncertainty to a degree. Commercial partners using TDRS as a source of launch vehicle tracking information were included, as were current operators of communications and imagery satellites and potential manned spaceflight providers. Finally, the Department of Defense was excluded as a stakeholder, based on information constraints. It is anticipated that national security stakeholders will be included in later classified variants of this effort.

Table 1. **Stakeholder list**

Stakeholder
NASA Earth Science
NASA Planetary Science
NASA Astrophysics Science
NASA Heliophysics Science
NASA Human Space Flight
NOAA GOES
NOAA POES
NOAA Oceanography
USGS Imagery
NSF Antarctic Program
International Partners
Commercial Partners (tracking)
Commercial Partners (imagery)

Previously, stakeholders network models were used to identify the relative priority of stakeholders. These models compute the value delivery to NASA by stakeholders (including potentially indirect paths) as a function of the transactions between stakeholders (network topology) and the stakeholders self-identified need strength. These models have the advantage of not explicitly requiring a prioritization of stakeholders, instead producing this prioritization as an output. The model described in this paper will initially use a prioritization among stakeholders, and will later evolve to compute stakeholder prioritization as a function of the network model.

The list of stakeholders is provided in Table 1. A three page stakeholder questionnaire was developed in order to populate the needs and satisfaction functions of the model, as well as to elicit potential other needs. Quantitative survey questions focus on data rates, latency, data volume per day (for each of science, housekeeping and forward services), type of tracking services and accuracy required. Additionally, qualitative questions are asked, including the stakeholders' relative priority of network FOMs (such as data rate, quality of service, data integrity, etc.), as well as their opinion of whether any of their requirements will drive or strongly influence the architecture.

To date, interviews have been conducted with nine stakeholder representatives, with data collection on going. In addition to these nine representatives, extensive consultation with existing TDRS operators has been conducted, as proxies for some of the stakeholders.

6. TRADESPACE MODELING

Architectural decisions

A SCAN architecture is modeled as the set of architectural decisions presented in Table 2. Thus, in order to fully

define an architecture, it is necessary to choose one option for each of the decisions shown in Table 2. In the rest of this subsection, each of these decisions is described in more detail.

Orbit and constellation design—The selection of the orbital parameters of the spacecraft, as well as the constellation parameters in case of a constellation, will largely determine the coverage of the constellation, i.e., the frequency and duration of accesses that can be provided to users in different orbital positions. It will also drive cost for several reasons:

1) Cost in general grows with the total number of spacecraft in the constellation

2) Launch cost per spacecraft strongly depends on orbital parameters through the ΔV required to achieve that orbit from a given launch site

3) The cost of a spacecraft also depends on orbital parameters, especially on orbit altitude, due to the varying effect of atmospheric drag, radiation, magnetic field, illumination conditions and so forth on the design of the spacecraft (see Section 6 for more details).

An orbit is perfectly defined by six parameters which can take continuous values; therefore there are in theory an infinity of different orbits. For the purposes of this architecting tool, only four families of orbits are considered, at least at this stage: Low Earth Orbit (LEO), Geostationary Earth Orbit (GEO), Medium Earth Orbit (MEO), and Highly Elliptical Orbit (HEO). While these are four canonical orbits representing infinite families of relatively similar orbits, a set of paradigmatic orbital parameters needs to be assumed for each one in order to make computations with them. These parameters are provided in Table 3.

In addition to the orbital parameters, it is necessary to define the constellation parameters. For LEO orbits, the tool assumes constellations of n_p planes of identical a, e, i, and ω, evenly distributed in Ω, and n_s satellites per plane, evenly distributed in mean anomaly. For the purpose of this piece of analysis, only $1 \leq n_p \leq 4$ and $1 \leq n_s \leq 4$ are considered. This yields a total of 4 options for orbit type, and 16 options for constellation design, i.e. 64 unconstrained options for orbit and constellation design, of which 12 are non-sensical because it is not possible to have $n_p > 1$ for GEO.

Design of communication payloads—The payload selection decision concerns the selection of the band and the types - and not the number - of communications payloads. The "type" of payload refers to the type of architecture implemented: bent-pipe vs circuit-switched vs packet-switched. The importance of this distinction depends strongly on specific characteristics of the traffic (e.g. its burstiness), as explained in the introduction. The current TDRS architecture is based on bent-pipe payloads, but the three options will be part of the tradespace for this study.

The band of the payload is important because it fixes most of the performance: data rates are largely driven by band selection. For example, high data rates beyond 512Mbps are only achievable by high bands (i.e. Ka or beyond). Legal considerations may also be important, as frequency allocation is severely controlled by international organisms. The payload selection decision has $2^{N_{bands}} - 1$ options, where N_{bands} is the number of bands that are being considered. Hence, for S-band, X-band, Ku-band, Ka-band, V-band, and optical, we have 63 options.

Payload-to-spacecraft allocation—The payload-to-spacecraft allocation decision concerns the allocation of the payloads to spacecraft, and therefore it depends on the payload selection decision (one cannot allocate payloads to satellites unless the payloads have been selected). Given that N_I payloads were selected in the payload selection decision, then $Bell(N_{instr})$ payload allocation options are available, where $Bell(i)$ indicates the ith Bell number, i.e., the number of partitions that can be done out of a set of i elements. For example, for a certain architecture with three payloads selected (S-band, Ka-band, optical), $N_{instr} = 3$, there are $Bell(3) = 5$ options for the payload-to-spacecraft allocation decision, namely:

$$\begin{aligned} A_1(3\ sats) &= \{\{S\},\{K_a\},\{optical\}\} \\ A_2(2\ sats) &= \{\{S,K_a\},\{optical\}\} \\ A_3(2\ sats) &= \{\{S\},\{K_a,optical\}\} \\ A_4(2\ sats) &= \{\{S,optical\},\{K_a\}\} \\ A_5(1\ sat) &= \{\{S,optical,K_a\}\} \end{aligned} \quad (1)$$

In the case of space communication networks, the payload allocation problem is mostly related to the cost of the architecture, and it is unlikely to affect its performance beyond the fact that payload have to share resources from a common bus, which they can do up to a certain level where the design of the bus becomes too costly or simply infeasible. The absence of positive and negative interactions between payloads (beyond those due to limitations of resources on the spacecraft) is a characteristic of communication systems, which does not hold in general for other systems. For instance, in Earth observation satellite systems, strong positive synergies or negative interferences often appear between instruments which may play a key role in the payload-to-spacecraft allocation problem [19].

Contract modality—The payloads and buses of the current TDRSS architecture were procured from commercial suppliers, and they are operated by NASA. In this approach, NASA retains most if not all of the control on the design and operation of the payload and the spacecraft. On the other hand, they have to pay for the whole cost of developing and fabricating the spacecraft (payloads and buses), testing, integrating, launching, and operating them.

Since then, alternative schemes have become available. The most notorious example is the "hosted payloads" approach, in which a spacecraft owner sells fractions of their spacecraft resources (mass, power, volume, data rate) to (usually) smaller secondary payloads. This approach has gained much popularity in recent years, with programs such as Iridium Next [20]. The reasons for its popularity are obvious: the hosted payload owner must only pay for the payload and a "service fee" that accounts for a fraction of the spacecraft development, fabrication, integration, testing, and launch costs. This "service fee" can be a function of a number of parameters including, but not limited to, the mass, power, and dimensions of the hosted payload. On the other hand, the hosted payload owner (i.e., NASA in this case), loses part of the control over the design and operation of the spacecraft. Exactly what part of the control is lost, and how costly is this "service fee" is still an open question as the first hosted payload contracts have only been signed in the last few years.

The concept of hosted payloads is an instance of a cost shar-

Table 2. Architectural decisions

Decision	Range of values	# options
Payload band selection	Any combination of the following: S-, X-, Ku-, Ka-, V-band and optical	$2^{N_{bands}} - 1 = 63$
Payload type selection	bent-pipe vs circuit-switched vs packet-switched	3
Payload-to-spacecraft allocation	All the possible partitions of N_{instr} instruments into $1 \leq N_{sat} \leq N_{instr}$ satellites	$Bell(N_{instr})$
Contract modality	100% procurement, hosted payloads, or 100% commercial	3
Orbit selection	GEO, HEO, MEO or LEO	4
Constellation design	#planes: 1-4 and #sats per plane 1-4	16

Table 3. Canonical orbit parameters

Orbit	Semimajor axis a(km)	Eccentricity e	Inclination i(deg)	RAAN Ω(deg)	Argument of the perigee ω(deg)	Mean anomaly ν(deg)
LEO	7178	0	90	0	0	0
GEO	42378	0	0	0	0	0
MEO	26378	0	90	0	0	0
HEO	42378	0.75	65	0	0	0

ing abstraction that can be generalized. This abstraction is as follows: let a proxy for the lifecycle cost of a communications constellation consists of payload cost, bus cost, launch cost, and operations cost. Then, the classic NASA procurement approach corresponds to a scheme where payload cost, bus cost, launch cost, and operations cost are all entirely paid for by NASA. Analogously, the hosted payloads approach corresponds to a scheme where NASA pays entirely for the payload cost, but only for a fraction of bus, launch, and operations cost. It is conceivable that other contract modalities can be devised that are hybrids of these approaches, as suggested in Table 4. In particular, there are $4^2 = 16$ different possible contract modalities, although arguably only a subset of these are plausible options. For example, it is unlikely that NASA would fully pay for the development of a next generation TDRS payload and bus and then let it be launched and operated by an external entity, however similar in nature this could be to what has happened in the Earth observation realm between NASA and NOAA.

After conversations with communications experts at NASA, it was decided to keep only options 0: 100% procurement, 7: hosted payloads, and 15: 100% commercial in the tradespace. The details of how the "service fee" is computed for all options (except for option 0 for which the service fee is 0 by definition) are provided in Section 6.

Architecture enumeration

The tool has the capability of automatically enumerating all the possible architectures defined by the decisions and options outlined in the previous section. If we consider the sets of options identified for each decision, the architectural tradespace is thus simply defined by the Cartesian product of all these sets. The size of this tradespace can be computed as:

$$N_{arc} = \sum_{N_{instr}=1}^{6} \binom{6}{N_{instr}} 468 Bell(N_{instr}) = 409968 \quad (2)$$

This means that almost 500,000 possible architectures for the SCaN program can be automatically enumerated and evaluated using this tool.

Performance model

The performance model intends to capture the ability of the network to satisfy a set of stakeholders given their relative importance and expected missions. It aims to (a) properly emulate the behavior of the network and (b) effectively capture how value is delivered to each stakeholder. Figure 1 presents the general structure of the performance model.

Modeling the network topology— The first step to model a space relay network is understanding the movement of both backbone nodes and end users over a representative period of time. This information is needed so as to define the contact opportunities between them and therefore assess when a particular path between an origin and a destination is available.

The performance model uses STK[9] in order to simulate the movement of both the space and ground segment. For each constellation, the following parameters can be input:

(1) Constellation design: number of planes, number of satellites per plane.

(2) Orbit design: altitude, eccentricity, inclination, argument of perigee.

(3) STK database: a list of satellite identifiers on the STK database ($SatId_1$, ..., $SatId_N$).

If (3) is specified then STK creates a constellation of satellites by directly importing their orbital information from the database ((1) and (2) are ignored). Otherwise, STK combines (1) and (2) to create a simplified constellation of equally spaced spacecraft both in latitude and longitude. The same process is followed in order to add the set of desired ground

[9] Satellite ToolKit AGI

Table 4. Contract modalities

Contract modality	Payload cost	Bus cost	Launch cost	Operations cost
Option 0: 100% procurement	Full	Full	Full	Full
Option 1	Full	Full	Full	Partial
Option 2	Full	Full	Partial	Full
...	...	...	...	...
Option 7: hosted payloads	Full	Partial	Partial	Partial
...	...	...	...	...
Option 15: 100% commercial	Partial	Partial	Partial	Partial

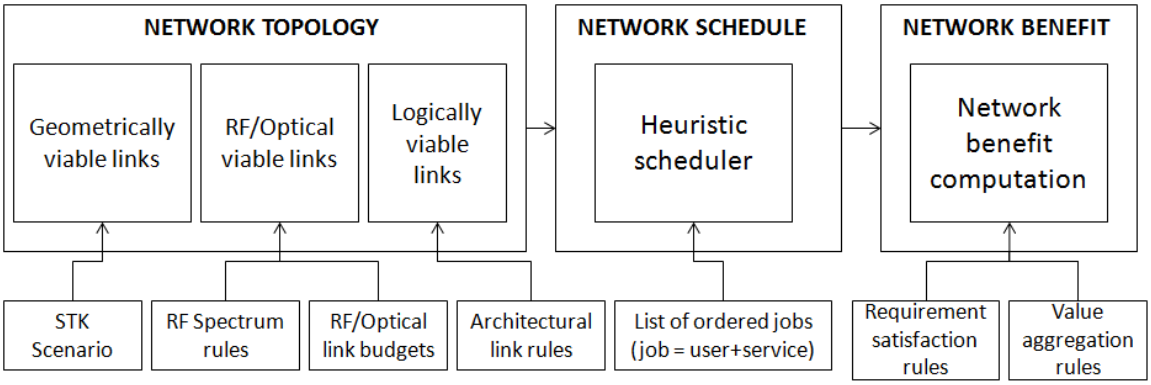

Figure 1. Structure of the performance model

stations. In this case, one can input their Earth coordinates or their STK database identifier.

Once all the nodes of the network have been put in place, the next step is to define the FOV of their antennas. This is done by appending sensors to each satellite and ground station and specifying their conical angle with respect to the nadir or zenith direction. Choosing between the nadir and zenith orientation is generally not trivial and depends on the relative position of the two communicating nodes. The model solves that problem by letting STK compute the four possible combinations (two for the transmitting antenna and two more for the receiving antenna) and automatically selecting the best one.

The output of the STK simulation is a set of reports that indicates the contact times between pairs of network nodes. These are parsed into a three dimensional binary matrix $C \in M_{NxNxT}$ where *N* indicates the number of network nodes and *T* the number of simulated time intervals (or snapshots). $C_{ijt} = 1$ indicates that node *i* is in line of sight with node *j* during time interval $[t, t + \Delta t]$. In turn, Δt is computed as

$$\Delta t = \frac{Total\ simulation\ time = \Delta T}{Number\ of\ time\ intervals = T} \tag{3}$$

STK is also used to compute the distances for contacts between nodes on the network. This information is used together with the communication payload transmitting power, modulation, coding and data rate as well as the antennae gain and G/T in order to calculate an estimate for all the link budgets. The result is again a binary three dimensional matrix $LB \in M_{NxNxT}$ that indicates if a particular link is viable at a given time interval. For communication payloads that do not have a specified transmitting frequency and bandwidth, a set of RF spectrum rules are used in order to determine them. Their goal is to encode the current ITU and NTIA regulations so as to ensure that a communication link is only possible if a given frequency band has some amount of bandwidth allocated for a particular type of link.

On the other hand, a set of rules is used in order to assess the communication links that are logically viable. For instance, a relay system based on a bent-pipe architecture like TDRSS does not have intersatellite links regardless of the relative position between spacecrafts. However, since both *C* and *LB* take only into consideration physical and RF/optical parameters, they might validate links between spacecrafts that are in field of view of each another and close enough to satisfy the link budget equations. In order to prevent that, the *link rules* determine what links are logically viable between two nodes of the network. The output of these rules is a two dimensional binary matrix $LL \in M_{NxN}$ where $LL_{ij} = 1$ indicates that link from node *i* to node *j* is logically viable. This *LL* matrix is repeated for all time intervals in order to obtain $LL \in M_{NxNxT}$.

Finally, once matrices *C*, *LB* and *LL* have been computed the overall network topology can be directly inferred as $NT = C\&LB\&LL$. This matrix will take into account the orbital mechanics of the nodes, the physical layer of the network and logical restrictions of the architecture so as to indicate the viable links at each time interval. As a result, it will capture the network topology at any instant in time.

Modeling the network schedule— The communication requirements for a particular mission depend both on its concept of operations and the demanded services. As an example, an Earth observation mission might require a science data

return service that intends to use three 5 minute contacts per orbit in order to return a total data volume of 200 GB/day. Alternatively, the International Space Station might require a video service four times a day with a duration of 15 minutes each contact.

In order to accommodate all the expected customers, a relay network has to determine how to optimally allocate its resources. This can be done through a scheduling algorithm that indicates what users and services will be supported at a given moment in time. This schedule is built taking into consideration at least three parameters:

- The network topology, i.e. what links are available at each moment of time. This information has already been computed and is stored in the matrix *NT*.

- The user and service priorities. They will indicate what users and services are more important and therefore must be scheduled first. This information is an input to the model.

- The concept of operations for a particular user and service: number of contacts, data volume to return per contact, minimum time between contacts. This information is an input to the model.

The current performance model has an especially built-in heuristic algorithm to emulate the scheduling process. Its high level structure is shown in figure 2.

It is assumed that a sorted list of required contacts is available at the start of the algorithm. This list is indexed through *k* and has the high priority jobs in the first positions. Therefore, if the scheduler tries to iteratively satisfy jobs in a descending priority order (*k=k+1*) then the most important will always be served first.

At each network snapshot *t* the network status must be computed. This is done by determining the amount of time that all links will be available and multiplying it by their current capacities. The result of this computation is a matrix *DV* capturing the data volume that can be returned given the current topology of the network. The link capacity used for this computations is not the nominal value but the remaining data rate given the connections that are already being supported. In other words, links that are physically viable but cannot support more services because they are already saturated are automatically neglected.

Once the network status has been computed, the next step is to try to schedule as many jobs as possible. The algorithm will use a shortest path algorithm to find a viable path between the user being serviced and a ground station of the network. In order to do so, a metric for costing a link L_{ij} must be specified.

$$Cost(L_{ij}) = \max\{DV_{ij} - \textit{data volume for the job}, 0\} \quad (4)$$

This definition ensures that the selected path minimizes the unused capacity of the network links. As a result, a telemetry service will always be routed through a set of low data rate links while a science return service will use a high data rate communication path. On the other hand, if a link does not have enough capacity to support a contact ($Cost(L_{ij}) < 0$) then it is directly invalidated ($Cost(L_{ij}) = 0$).

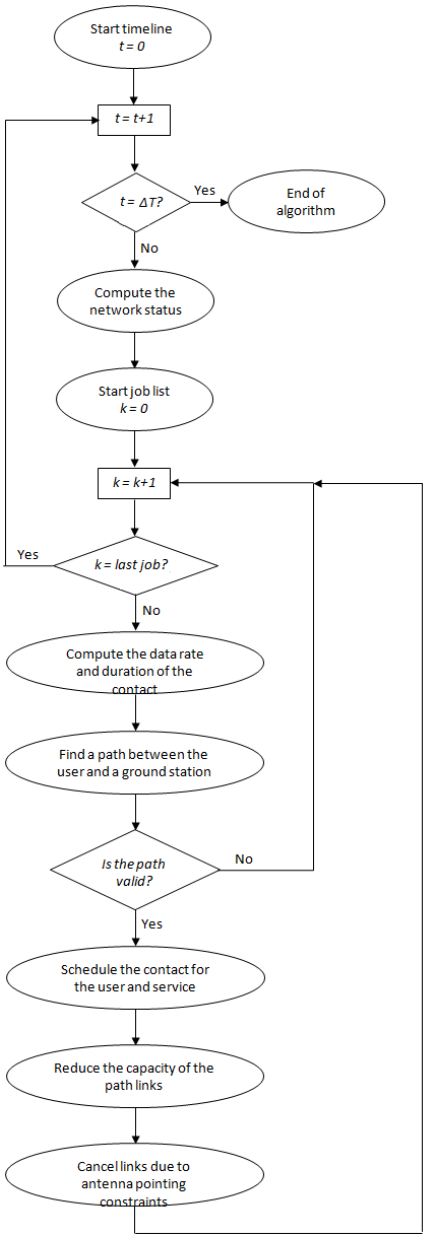

Figure 2. Heuristic scheduling algorithm

With this approach, a service with a viable path from the user to a ground station is automatically selected for schedule. When that happens, three main actions take place:

- Information regarding the instant times during which a particular job has been served gets stored. This information can be later processed to graphically represent the obtained schedule for any user of the network.
- The capacities of the links on the selected path decrease by the service data rate. It is assumed that there is no channelization of the link bandwidth and therefore the amount of retractable data rates is not discretized.
- Links that were previously viable become unfeasible due to beam pointing constraints. These links are only invalidated for the duration of the scheduled contact.

Modeling the network traffic— The current performance model neglects the burstiness of the traffic that flows through

the network. In fact, data rates to support a service are always computed as averages in this model.

$$R_b = \frac{data\ volume}{contact\ time} \tag{5}$$

This assumption might hold under scenarios where the traffic source sends data at a constant bit rate (CBR) and the transport, network and data link protocols add little overhead, redundancy and control information.

A more realistic approach would consider that each service has different traffic characteristics. [21] presents a comprehensive study on video, voice, telemetry and command services on past NASA missions. Its results indicate that the data rate for supporting these services can in fact be modeled through gamma distributions. A similar conclusion is presented in [22] for IP traffic over space networks. It also presents an analytic solution for determining the gain of using packet-based architectures that statistically multiplex the incoming traffic.

Incorporating these result to the performance model will be done in future versions of the tool. They will allow to increase the accuracy of the heuristic scheduler and ensure that link do not get overloaded due to the traffic burstiness. They will also allow to numerically assess the differences between packet and circuit-switched architectures.

Computing the architecture benefit—Once the network schedule has been computed, determining the benefit of the architecture can be easily done through a two step process.

- The fraction of successfully scheduled contacts is compared to the expectations of each mission through the *requirement satisfaction rules*. They encode the satisfaction that the user has given the performance of the system. As an example, an Earth Observation mission that can only schedule 50% of its desired contacts might be completely unsatisfied because half of the collected data cannot be returned.
- The satisfaction of all missions are aggregated for the objectives and stakeholders through the *value aggregation rules*. They compute the weighted sum of the user, objective and stakeholder satisfaction in order to assess the benefit of the whole architecture. The relative importance or weights for the *value aggregation rules* must be known beforehand and are an input to the model.

Cost model

The goal of the cost model is to provide an estimate of the lifecycle cost of an architecture (i.e., a set of constellations and ground stations) that is good enough for relative comparison across architectures. This includes in particular differentiating between different contract modalities, (procurement vs hosted payloads vs 100% commercial).

The lifecycle cost estimate consists of several parts: payload cost, bus cost, launch cost, IA&T cost, operations cost, and program overhead. Some of these are further divided into non-recurring and recurring costs, as illustrated in Fig. 3.

Payload Cost—Payload cost is only incurred when the contract modality is procurement or hosted payloads. If a 100% commercial approach is taken, payload cost is set to zero, as it is included in the service fee charged to NASA by the provider. Payload cost is the sum of a non-recurring cost and a recurring cost. When these values are not provided by the user, they are estimated using CERs that utilize payload mass m and number of channels n as independent variables. The CERs are taken from the USCM8 model [23] and are provided below. All values are in FY2010$k.

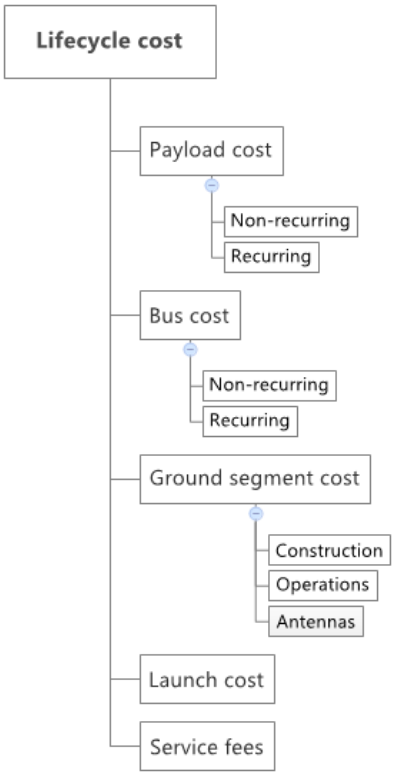

Figure 3. Lifecycle cost breakdown

$$C_{payl,NR} = 339m + 5127n \tag{6}$$

$$C_{payl,R} = 189m \tag{7}$$

where $C_{payl,NR}$ is the development cost including the cost of fabricating a qualification unit and $C_{payl,R}$ is the cost of fabricating the first flight unit. The standard error of the estimate (SEE) of Equation 6 inside the domain 160-395kg and 2-32 channels is 40%. The SEE of Equation 7 inside the domain 38-928kg is 28%. All SEEs are corrected for the number of degrees of freedom. Total cost for development and fabrication of N identical payloads is thus given by:

$$C_{payl} = C_{payl,NR} + N^b C_{payl,R} \tag{8}$$

where $b < 1$ is chosen to model a cumulative average learning curve of 95%.

Bus Cost— Bus cost is only incurred when the contract modality is procurement. If a 100% commercial approach or hosted payloads approach are taken, bus cost is set to zero, as it is included in the service fee charged to NASA by the provider. Bus cost is the sum of a non-recurring cost and a recurring cost. When these values are not provided by the

user, they are estimated using CERs that utilize subsystem mass as the independent variable. The CERs are taken from the USCM8 model [23] and are provided below. All values are in FY2010$k.

$$C_{bus,NR} = 110.2 m_{dry} \tag{9}$$

$$C_{bus,R} = 289.5 m_{dry}^{0.716} \tag{10}$$

where m_{dry} is the satellite dry mass, $C_{bus,NR}$ is the development cost including the cost of fabricating a qualification unit and $C_{payl,R}$ is the cost of fabricating the first flight unit. The standard error of the estimate (SEE) of Equation 9 inside the domain 114-5127kg is 47%. The SEE of Equation 10 inside the domain 288-7398kg is 21%. Total cost for development and fabrication of N identical buses is computed as illustrated in Equation 8, with a learning factor of 95%. Note that the computation of bus cost depends on the dry mass of the spacecraft. This can be provided by the user, or it can be estimated by the spacecraft design module, which is described later in this section.

Launch Cost—Launch cost is only incurred when the contract modality is procurement. If a 100% commercial approach or hosted payloads approach are taken, launch cost is set to zero, as it is included in the service fee charged to NASA by the provider. Launch cost is given by the sum of the costs of launching all constellations in the architecture. Computation of launch cost for a constellation is based on the assumption that, given a constellation of P planes and S satellites per plane, $P < N_L < PS$ launches are necessary to launch the constellation, i.e., at least one launch per plane (in other words, satellite engines are not sized to do inclination changes after injection), and at most one launch per satellite. The exact value of N_L is obtained by taking into account both performance and geometrical considerations.

In particular, a database of launchers is available to each constellation. This database is shown in Table 5. Note that the data concerning performance is provided in terms of the 3 coefficients of a quadratic function of the orbit altitude. In other words, if the entry of the table for a certain orbit type (e.g., LEO polar) gives the coefficients $[a, b, c]$, then the performance at altitude h can be computed as :

$$perf(h) = a + bh + ch^2 \tag{11}$$

Given these data, N_L is computed as follows:

$$N_L = \max\{N_{L,mass}, N_{L,vol}, N_{L,dim}\} \tag{12}$$

where $N_{L,mass}$ is the minimum number of launches required given the total spacecraft mass and the performance of the launch vehicle to the desired orbit; $N_{L,vol}$ is the minimum number of launches required given the total spacecraft volume and the volume of the launch vehicle; $N_{L,dim}$ is the minimum number of launches required given the sum of the maximum dimension of all spacecraft and the height of the launch vehicle:

$$N_{L,mass} = \lceil \frac{\sum_{i=1}^{N_{S/C}} m_{wet,i}}{perf(lv, orbit)} \rceil \tag{13}$$

$$N_{L,vol} = \lceil \frac{\sum_{i=1}^{N_{S/C}} vol_i}{vol_{lv}} \rceil \tag{14}$$

$$N_{L,diam} = \lceil \frac{\sum_{i=1}^{N_{S/C}} dmax_i}{h_{lv}} \rceil \tag{15}$$

where $N_{S/C}$ is the number of spacecraft in the constellation, $m_{wet,i}$, vol_i, and $dmax_i$ are the wet mass, volume, and maximum dimension respectively of spacecraft i, and $perf(lv, orbit)$, vol_{lv}, and h_{lv} are the performance at the desired orbit, the volume, and the height respectively of the launch vehicle. Once the number of launches has been computed, launch cost is simply given by the product of number of launches and launch cost.

Ground segment cost—Ground segment cost is the sum of a non-recurring cost and a recurring cost. When these values are not provided by the user, they are estimated using CERs that utilize location of the facility, the number of spacecraft, and spacecraft lifetime as independent variables. The CERs are taken from [23] and are provided below. All values are in FY2010$k.

$$C_{ground,R} = C_{ground,NR} + C_{ground,R} t(yr) = \\ = F(loc) 6,471 (\frac{\$}{m^2}) A(m^2) + 0.5 \frac{\$M}{S/C/yr} N_{S/C} t(yr) \tag{16}$$

where $F(loc)$ is an adjustment factor that takes into account differences in construction cost in different locations, A is the floor area of the facility in m^2, and $t(yr)$ is the lifetime in years. The values of the adjustment factor are taken from [23].

Service fees— Service fees are only applicable for hosted payloads and 100% commercial approaches. In these cases, they can replace payload, bus, launch, or ground segment cost. Service fees for the hosted payloads approach are computed as a fix quantity (10$M) per hosted payload 'slot', where a 'slot' is defined by the satellite operator in terms of resources such as volume, mass, power, data rate, or a combination thereof. Service fees for the 100% commercial approach are computed as a fixed quantity ($2k) per Tb of data transmitted.

Spacecraft design—The spacecraft design module can be bypassed by choosing to assign a commercially available bus instead of designing a bus. While the standard bus approach is closer to reality, the spacecraft design module provides more distinction in lifecycle cost between different architectures, and therefore it is chosen as the primary operating mode of the tool. The spacecraft design module is an iterative module that provides a subsystem-level design of the spacecraft bus including a very rough configuration of the spacecraft from the payload requirements.Assumptions concerning the different sub-modules in the spacecraft design module, namely the bus selection module and the four steps of the process shown

Table 5. **Extract of launch vehicle database**

	Atlas-V	**Delta-7920**	**Taurus-XL**
Payload GTO	[10^4,0,0]	[$5 \cdot 10^2$,0,0]	[0,0,0]
Payload LEO polar	[$15 \cdot 10^3$,$-4 \cdot 10^{-2}$,0]	[$4 \cdot 10^3$,$-1 \cdot 10^{-2}$,$7 \cdot 10^{-5}$]	[$1.2 \cdot 10^3$,$-4.4 \cdot 10^{-2}$,0]
Diameter (m)	4.8	2.7	2.0
Height (m)	10.0	7.53	5.71
Cost (FY2010$M)	100	65	30

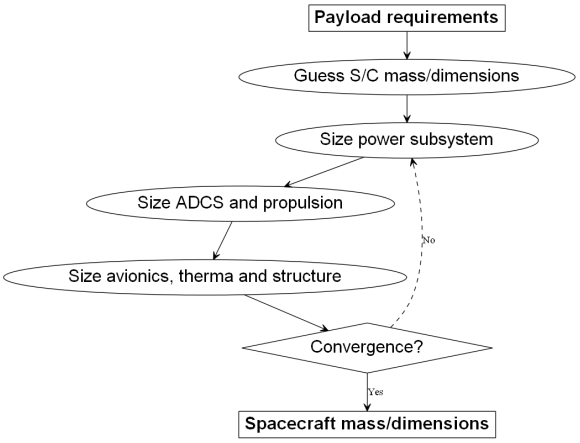

Figure 4. Spacecraft design algorithm

in Figure 4are described in detail in the rest of this section.

Electrical power subsystem design— The Electrical Power Subsystem (EPS) is designed based on a very rough power budget. The mass of the EPS is given by:

$$m_{EPS} = m_{SA} + m_{batt} + m_{other} \tag{17}$$

where m_{SA} is the mass of the solar array, m_{batt} is the mass of the batteries, and m_{other} is the mass of the other components. The solar array is designed to provide enough power at end-of-life, assuming a certain yearly degradation $\eta(\%/yr)$. Its mass is calculated assuming a given specific power $\rho_p(W/kg)$:

$$\begin{aligned} P_{SA}(W) &= \frac{P_e \frac{T_e}{X_e} + P_d \frac{T_d}{X_d}}{T_d} \\ W_{BOL}(\frac{W}{m^2}) &= W_0 I_d \cos\theta \\ A_{SA}(m^2) &= \frac{P_{SA}}{W_{BOL}(1-\eta)^t} \\ m_{SA}(kg) &= \frac{W_{BOL} A_{SA}}{\rho_p} \end{aligned} \tag{18}$$

where $T_e(s)$ is the average eclipse time per orbit, which is calculated from geometrical considerations, $T_d(s) = T - T_e$, $T(s)$ is the orbital period, $P_e(W)$ are the power requirements during eclipse, $P_d(W)$ are the power requirements during daylight, X_d and X_e are the energetic efficiencies between the solar array and the power bus (through the batteries in case of eclipse), $W_0(W/m^2)$ is the power density given by the solar array technology, I_d is an efficiency, θ is the Sun angle, $W_{BOL}(\frac{W}{m^2})$ is the power density of the solar array at BOL, and $A_{SA}(m^2)$ is the solar array area.

The mass of the batteries is calculated from its capacity assuming a certain specific energy $\rho_e(Wh/kg)$:

$$\begin{aligned} C_r(Wh) &= \frac{P_e T_e}{3600 DOD n} \\ m_{batt}(kg) &= \frac{C_r}{\rho_e} \end{aligned} \tag{19}$$

where DOD is the depth of discharge (which depends on the orbital parameters) and n is the efficiency from the batteries to the load. In particular, the DOD is assumed to be 0.8 for GEO, 0.6 for dawn-dusk SSO, and 0.4 for all other orbits.

The mass of the rest of components (regulators, converters, and wiring) is estimated as a function of the power at beginning of life P_{BOL} and the spacecraft dry mass m_{dry} as suggested in [24]:

$$m_{other} = \alpha P_{BOL} + \beta m_{dry} \tag{20}$$

where: α has a component of regulated power and a component of converted power, $P_{BOL} = W_{BOL} A_{SA}$ is the power available at BOL, β accounts for wiring, and m_{dry} is the spacecraft dry mass.

Delta-V and propellant mass budgets— The design of the ADCS and propulsion subsystems is based on a rough ΔV budget of the spacecraft, which consists of four components: injection, drag compensation, ADCS, and deorbiting:

$$\Delta V = \Delta V_{inj} + \Delta V_{drag} + \Delta V_{ADCS} + \Delta V_{deorbit} \tag{21}$$

The ΔV_{inj} is computed assuming that the spacecraft is injected into a transfer orbit that has the perigee at 150km and the apogee at the final orbit altitude:

Table 6. ΔV **required to compensate drag for different orbits**

Orbit	$\Delta V_{drag}(m/s/yr)$
LEO($h < 500km$)	12
LEO($500km < h < 600km$)	5
LEO($600km < h < 1000km$)	2
MEO	0
GEO	0
HEO	0

Table 7. ΔV **required for ADCS**

ADCS configuration	$\Delta V_{ADCS}(m/s/yr)$
Three-axis	20
Spinner	0
Gravity gradient	0

$$V(r_p, r_a, r) = \sqrt{2\mu(\frac{1}{r} - \frac{1}{r_p + r_a})}$$
$$\Delta V(r_{p1}, r_{a1}, r_{p2}, r_{a2}, r) =$$
$$= |V(r_{p2}, r_{a2}, r) - V(r_{p1}, r_{a1}, r)|$$
$$\Delta V_{inj} = \Delta V(R_E + 150km, r, r, r, r) \quad (22)$$

where $\Delta V(r_{p1}, r_{a1}, r_{p2}, r_{a2}, r)$ is the ΔV necessary to perform a change of orbit semimajor axis from orbit (r_{p1}, r_{a1}) to orbit (r_{p2}, r_{a2}) when the spacecraft is at distance r from the Earth.

The ΔV_{drag} necessary to compensate drag is strongly dependent on orbit altitude. The values shown in Table 6 were taken from [25]:

The ΔV_{ADCS} required for ADCS depends on the ADCS configuration, as shown in Table 7. These values were adapted from [25].

The $\Delta V_{deorbit}$ is computed assuming that LEO spacecraft are deorbited using atmospheric drag, and all other spacecraft are deorbited using solar radiation presure. For drag-based deorbiting, the$\Delta V_{deorbit}$ is computed based on a change of semimajor axis from the current circular orbit to an elliptical orbit that has the perigee at 0km and the apogee at the orbit altitude:

$$\Delta V_{deorbit,drag} = \Delta V(r, r, R_E, r, r) \quad (23)$$

For solar radiation pressure-based deorbiting, the$\Delta V_{deorbit}$ is computed based on a change of semimajor axis from the current circular orbit to an elliptical orbit that has the same perigee and a slightly higher apogee:

$$\Delta V_{deorbit,SRP} = \Delta V(r, r, r, r + \Delta h, r)$$
$$\Delta h = 200km + 35km + \frac{1000 C_R A}{m_{dry}} km \quad (24)$$

where the 200km are due to the GEO restricted zone, the 35km are to allow for gravitational perturbations, and the remaining margin depends on the magnitude of the effect of solar radiation pressure on the spacecraft (the larger the effect, the larger the margin); C_R is the solar radiation pressure coefficient, and A is the surface area of the spacecraft.

Once the ΔV has been calculated, it is possible to compute the propellant mass required to satisfy this ΔV budget. The tool assumes that ΔV_{inj} is performed by the apogee kick motor (AKM), while the other ΔV are performed by the ADCS subsystem. For each of these propulsion systems, the propellant mass can be computed using the rocket equation:

$$\Delta V_j = g I_{sp,j} \log \frac{m_i}{m_f} \quad (25)$$

where I_{sp} is the propelllant specific impulse, which can be different for the AKM and the ADCS subsystem, m_i is the initial mass with propellant and m_f is the final mass without the propellant.

Attitude Determination and Control and Propulsion Subsystem—The mass of the ADCS is mostly given by the mass of the sensors and the mass of the actuators. The mass of the sensors is driven by the attitude knowledge accuracy requirement acc (Equation 26), while the actuators are sized to satisfy by the momentum storage h required (Equation 27):

$$m_{sen} = 10 acc^{-0.316} \quad (26)$$

$$m_{act} = 1.5 h^{0.6} \quad (27)$$

Note that acc can vary depending on the architecture, as the pointing requirements of a high gain antenna, or an optical payload, are very different from those of a low gain antenna. Concerning the momentum storage h, it is assumed to be sized to counter the different disturbance torques produced by atmospheric drag, gravity gradient, solar radiation pressure, or the Earth's magnetic field. Expressions for these disturbance torques were taken from [25].

In addition to sensors and actuators, the ADCS has additional mass that can be estimated as a fix fraction of the spacecraft dry mass:

$$m_{ADCS} = 3 m_{sen} + 4 m_{act} + 0.01 m_{dry} \quad (28)$$

Concerning the propulsion subsystem, the mass of the AKM can be estimated from its propellant mass assuming a certain mass fraction:

$$m_{AKM} = \frac{(1 - \mu)}{\mu} m_{prop,inj} \quad (29)$$

Table 8. Coefficients used in CERs for thermal, avionics, and structure subsystem

Subsystem	k
Thermal	0.0607
Avionics	0.0983
Structure	0.5462

Thermal, avionics, and structure subsystems—The thermal, avionics, and structure subsytems are designed using simple parametrics of the form $m_{subsystem} = km_{payload}$. The constans k that are used for each subsystem are summarized in Table 8.

The mass of the launch adapter $m_{LA} = 0.01m_{dry}$ is added to the mass of the spacecraft.

Update spacecraft mass and dimensions—After the first iteration, the dry and wet mass of the spacecraft are updated. Dimensions are estimated assuming a perfect cube of 100 kg/m^3. The mass and dimensions of the solar panels are taken into account to update the inertial properties of the spacecraft, as illustrated in Equation 30:

$$\begin{aligned} L_A &= 1.5s + 0.5\sqrt{\frac{A_a}{2}} \\ I_z &= 0.01m_{dry} \\ I_x = I_y &= I_z + L_a^2 M_a \end{aligned} \tag{30}$$

Convergence criteria— The spacecraft design algorithm is iterative because several feedback loops appear in the N^2 matrix showing the dependences between different modules in the algorithm. For instance, the mass of the ADCS depends on the mass of the spacecraft, which obviously depends on the mass of the ADCS. Thus, a set of convergence criteria need to be defined. The convergence criteria used by the tool are described in Equation 31:

$$|m_{dry,i+1} - m_{dry,i}| < 10kg \tag{31}$$

where the subscript i indicates the number of iteration.

7. CONCLUSION

Summary

This paper has presented the current status of the MIT architecture study for the SCaN system. The study consists of a stakeholder analysis to identify the primary stakeholders and their needs, and the development of a computational tool to explore the architectural tradespace.

Several interviews have been conducted with experts at NASA to elicit the potential requirements on SCaN from different user communities.

The major architectural decisions to be made by the SCaN program have been identified and encoded in a mathematical model. A computational tool has been developed that can automatically enumerate and evaluate thousands of different SCaN architectures. This tool contains both a performance and a cost model.

Next Steps

The next steps include calibration of the optical link budget calculations, comparisons of the network scheduling calculations with historical TDRSS load data, and validation of the spacecraft sizing algorithm with real TDRS data. Following the completion of the stakeholder analysis, the tool will be be used to explore the architectural tradespace and identify a subset of preferred architectures worth studying in more detail. These architectures could then be analyzed in NASA's Architecture Development Lab (ADL).

ACKNOWLEDGMENTS

This project is funded by NASA under grant #NNX11AR70G. The authors would also like to thank the *Centre de Formacio Interdisciplinària Superior* and the *Cellex* Foundation for partially funding this project.

REFERENCES

[1] S. Tsiao, *Read you loud and clear! The story of NASA's spaceflight tracking and data network*. Washington DC: Library of Congress, 2007.

[2] G. Maral, *Satellite Communication Systems: systems, techniques and technology*, 2009.

[3] K. Y. Jo, "Satellite communications with Internet Protocol (IP) efficiency," *MILCOM 2009 - 2009 IEEE Military Communications Conference*, pp. 1–7, Oct. 2009.

[4] E. Jennings and D. Heckman, "Architecture Modeling and Performance Characterization of Space Communications and Navigation (SCaN) Network Using MACHETE."

[5] E. Jennings, R. Borgen, S. Nguyen, J. Segui, T. Stoenescu, S.-y. Wang, and S. Woo, "Space Communications and Navigation (SCaN) Network Simulation Tool Development and Its Use Cases," *American Institute of Aeronautics and Astronautics*, no. August, pp. 1–11, 2009.

[6] E. Jennings and D. Heckman, "Performance Characterization of Space Communications and Navigation (SCaN) Network by Simulation," *2008 IEEE Aerospace Conference*, pp. 1–9, Mar. 2008.

[7] J. Alonso and K. Fall, "A Linear Programming Formulation of Flows over Time with Piecewise Constant Capacity and Transit Times piecewise constant capacity and transit times," 2003.

[8] B. L. Murphy, "High Resolution Satellite Communication Simulation," 2000.

[9] M. Werner, A. Jahn, E. Lutz, and A. Bottcher, "Analysis of System Parameters for LEO/ICO-Satellite Communication Networks," 1995.

[10] T. Weilkiens, *Systems engineering with SysML/UML: modeling, analysis, design*. Heidelberg, Germany: The Morgan Kaufmann/OMG Press, 2006.

[11] M. Rao, S. Ramakrishnan, and C. Dagli, "Modeling and Simulation of Net Centric System of Systems Using Systems Modeling Language and Colored Petri-nets : A Demonstration Using the Global Earth Observation

System of Systems," *Systems Engineering*, vol. 11, no. 3, pp. 203–220, 2008.

[12] B. H. Y. Koo, W. L. Simmons, and E. F. Crawley, "Algebra of Systems: A Metalanguage for Model Synthesis and Evaluation," *IEEE Transactions on Systems, Man, and Cybernetics - Part A: Systems and Humans*, vol. 39, no. 3, pp. 501–513, May 2009.

[13] M. Ehrgott and X. Gandibleux, "A Survey and Annotated Bibliography of Multiobjective Combinatorial Optimization," *OR Spectrum*, vol. 22, no. 4, pp. 425–460, Nov. 2000.

[14] D. Selva, "Rule-based system architecting of Earth observation satellite systems," PhD dissertation, Massachusetts Institute of Technology, 2012.

[15] D. Selva and E. F. Crawley, "VASSAR: Value Assessment of System Architectures using Rules," in *Proceedings of the 2013 IEEE Aerospace Conference*, Big Sky, Montana, 2013.

[16] T. Sutherland, B. Cameron, and E. Crawley, "Program goals for the nasa/noaa earth observation program derived from a stakeholder value network analysis," 2012.

[17] B. Cameron, E. Crawley, G. Loureiro, and E. Rebentisch, "Value flow mapping: Using networks to inform stakeholder analysis," *Acta Astronautica*, vol. 62, pp. 324–333, 2008.

[18] B. Cameron and Crawley, "Goals for space exploration based on stakeholder network value considerations," *Acta Astronautica*, vol. 68, pp. 2088–2097, 2011.

[19] D. Selva and E. F. Crawley, "Integrated Assessment of Packaging Architectures in Earth Observing Programs," in *Proceedings of the 2011 IEEE Aerospace Conference*, Big Sky, Montana, 2010.

[20] O. P. Gupta and C. S. Fish, "Iridium NEXT: A Global access for your sensor needs," in *Proceedings of the 2010 American Geophysical Union Fall Meeting*, San Francisco, CA, 2010.

[21] T. Stoenescu and L. Clare, "Traffic Modeling for NASA's Space Communications and Navigation (SCaN) Network," in *2008 IEEE Aerospace Conference*, Mar. 2008, pp. 1–14.

[22] K. Y. Jo, "Satellite communications with Internet Protocol (IP) efficiency," *MILCOM 2009 - 2009 IEEE Military Communications Conference*, pp. 1–7, Oct. 2009.

[23] H. Apgar, "Cost Estimating," in *Space Mission Engineering: The new SMAD*. Hawthorne, CA: Microcosm, 2011, ch. 11.

[24] R. S. Bokulic, C. C. DeBoy, S. W. Enger, J. P. Schneider, and J. K. McDermott, "Spacecraft Subsystems IV Communications and Power," in *Space Mission Engineering: The new SMAD*. Hawthorne, CA: Microcosm, 2011, ch. 21.

[25] P. Springmann and O. de Weck, "Parametric scaling model for nongeosynchronous communications satellites," *Journal of spacecraft and rockets*, vol. 41, no. 3, pp. 472–477, 2004.

BIOGRAPHY

Marc Sanchez *is a senior student from Universitat Politecnica de Catalunya (Barcelona, Spain) working towards B.S. and M.S. degrees in Mechanical Engineering and Telecommunications Engineering. His is currently a Visiting Student at the Space System Architecture Group of MIT, focusing his interests in rule-based expert systems and how they can be applied to space communications networks. Prior to his work at MIT, Marc has been a software engineer at Sener Ingenieria y Sistemas involved in the development of commercial software FORAN CAD/CAM.*

Dr. Daniel Selva *received a PhD in Space Systems from MIT in 2012 and he is currently a post-doctoral associate in the department of Aeronautics and Astronautics at MIT. His research interests focus on the application of multidisciplinary optimization and artificial intelligence techniques to space systems engineering and architecture, in particular in the context of Earth observation missions. Prior to MIT, Daniel worked for four years in Kourou (French Guiana) as a member of the Ariane 5 Launch team. In particular, he worked as a specialist in operations concerning the guidance, navigation and control subsystem, and the avionics and ground systems. Daniel has a dual background in electrical engineering and aeronautical engineering, with degrees from Universitat Politecnica de Catalunya in Barcelona, Spain, and Supaero in Toulouse, France. He is a 2007 la Caixa fellow, and received the Nortel Networks prize for academic* excellence in 2002.

Dr. Bruce Cameron *is a Lecturer in Engineering Systems at MIT and a consultant on platform strategies. At MIT, Dr. Cameron ran the MIT Commonality study, a 16 firm investigation of platforming returns. Dr. Cameron's current clients include Fortune 500 firms in high tech, aerospace, transportation, and consumer goods. Prior to MIT, Bruce worked as an engagement manager at a management consultancy and as a system engineer at MDA Space Systems, and has built hardware currently in orbit. Dr. Cameron received his undergraduate degree from the University of Toronto, and graduate degrees from MIT.*

Dr. Edward F. Crawley *received an Sc.D. in Aerospace Structures from MIT in 1981. His early research interests centered on structural dynamics, aeroelasticity, and the development of actively controlled and intelligent structures. Recently, Dr. Crawleys research has focused on the domain of the architecture and design of complex systems. From 1996 to 2003 he served as the Department Head of Aeronautics and Astronautics at MIT, leading the strategic realignment of the department. Dr. Crawley is a Fellow of the AIAA and the Royal Aeronautical Society (UK), and is a member of three national academies of engineering.*

He is the author of numerous journal publications in the AIAA Journal, the ASME Journal, the Journal of Composite Materials, and Acta Astronautica. He received the NASA Public Service Medal. Recently, Prof Crawley was one of the ten members of the presidential committee led by Norman Augustine to study the future of human spaceflight in the US.

Bernard D. Seery *is the Assistant Director for Advanced Concepts in the Office of the Director at NASA's Goddard Space Flight Center (GSFC). Responsibilities include assisting the Deputy Director for Science and Technology with development of new mission and measurement concepts, strategic analysis, strategy development and investment resources prioritization. Prior assignments at NASA Headquarters included Deputy for Advanced Planning and Director of the Advanced Planning and Integration Office (APIO), Division Director for Studies and Analysis in the Program Analysis and Evaluation (PA&E) office, and Deputy Associate Administrator (DAA) in NASA's Code U Office of Biological and Physical Research (OBPR). Previously, Bernie was the Deputy Director of the Sciences and Exploration Directorate, Code 600, at (GSFC). Bernie graduated from Fairfield University in Connecticut in 1975 with a bachelors of science in physics, with emphasis in nuclear physics. He then attended the University of Arizona's School of Optical Sciences, and obtained a masters degree in Optical Sciences, specializing in nonlinear optical approaches to automated alignment and wavefront control of a large, electrically-pumped CO2 laser fusion driver. He completed all the course work for a PhD in Optical Sciences in 1979, with emphasis in laser physics and spectroscopy. He has been a staff member in the Laser Fusion Division (L-1) at the Los Alamos National Laboratories (LANL), managed by the University of California for the Department of Energy, working on innovative infrared laser auto-alignment systems and infrared interferometry for target alignment for the HELIOS 10 kilojoule, eight-beam carbon dioxide laser fusion system. In 1979 he joined TRW's Space and Defense organization in Redondo Beach, CA and designed and developed several high-power space lasers and sophisticated spacecraft electro-optics payloads. He received the TRW Principal Investigators award for 8 consecutive years.*

Dr. Antonios A. Seas *is a Study Manager at the Advanced Concept and Formulation Office (ACFO) of the NASA's Goddard Space Flight Center. Prior to this assignment he was a member of the Lasers and Electro-Optics branch where he focused on optical communications and the development of laser systems for space applications. Prior to joining NASA in 2005 he spent several years in the telecommunication industry developing long haul submarine fiber optics systems, and as an Assistant Professor at the Bronx Community College. Antonios received his undergraduate and graduate degrees from the City College of New York, and his doctoral degree from the Graduate Center of the City University of New York. He is also a certified Project Management Professional.*